SANDIA REPORT

SAND2012-7645
Unlimited Release
Printed September 2012

The Verification and Uncertainty Quantification of Surrogate Models Used for Structural Analysis

Michael Ross, Angel Urbina, Todd Simmermacher, Thomas Paez

Prepared by
Sandia National Laboratories
Albuquerque, New Mexico 87185 and Livermore, California 94550

Sandia National Laboratories is a multi-program laboratory managed and operated by Sandia Corporation, a wholly owned subsidiary of Lockheed Martin Corporation, for the U.S. Department of Energy's National Nuclear Security Administration under contract DE-AC04-94AL85000.

Approved for public release; further dissemination unlimited.

Sandia National Laboratories

Issued by Sandia National Laboratories, operated for the United States Department of Energy by Sandia Corporation.

NOTICE: This report was prepared as an account of work sponsored by an agency of the United States Government. Neither the United States Government, nor any agency thereof, nor any of their employees, nor any of their contractors, subcontractors, or their employees, make any warranty, express or implied, or assume any legal liability or responsibility for the accuracy, completeness, or usefulness of any information, apparatus, product, or process disclosed, or represent that its use would not infringe privately owned rights. Reference herein to any specific commercial product, process, or service by trade name, trademark, manufacturer, or otherwise, does not necessarily constitute or imply its endorsement, recommendation, or favoring by the United States Government, any agency thereof, or any of their contractors or subcontractors. The views and opinions expressed herein do not necessarily state or reflect those of the United States Government, any agency thereof, or any of their contractors.

Printed in the United States of America. This report has been reproduced directly from the best available copy.

Available to DOE and DOE contractors from
U.S. Department of Energy
Office of Scientific and Technical Information
P.O. Box 62
Oak Ridge, TN 37831

Telephone: (865) 576-8401
Facsimile: (865) 576-5728
E-Mail: reports@adonis.osti.gov
Online ordering: http://www.osti.gov/bridge

Available to the public from
U.S. Department of Commerce
National Technical Information Service
5285 Port Royal Rd
Springfield, VA 22161

Telephone: (800) 553-6847
Facsimile: (703) 605-6900
E-Mail: orders@ntis.fedworld.gov
Online ordering: http://www.ntis.gov/help/ordermethods.asp?loc=7-4-0#online

SAND2012-7645
Unlimited Release
Printed September 2012

The Verification and Uncertainty Quantification of Surrogate Models Used for Structural Analysis

Michael Ross, Angel Urbina, Todd Simmermacher
Sandia National Laboratories
P.O. Box 5800
Albuquerque, NM 87185-0828

Thomas Paez
Thomas Paez Consulting
Durango, CO 80301

Abstract

High fidelity modeling of complex systems can require large finite element models to capture the physics of interest. Typically these high-order models take an excessively long time to run. For important studies such as model validation and uncertainty quantification, where probabilistic measures of the response are required, a large number of simulations of the high fidelity model with different parameters are necessary. In addition, some environments, such as an extensive random vibration excitation, require a long simulation time to capture the entire event. A process that produces a highly efficient model from the original high order model is necessary to enable these analyses. These highly efficient models are referred to as surrogate models, for their purpose is to represent the main physics that is of importance, but decrease the computational burden. A critical aspect of any surrogate model is how faithfully the efficient model represents the original high-order model. This paper describes the process for verifying a surrogate model using response quantities of interest and quantifying the introduced uncertainties in the use of the surrogate model. This is done to help any analyst if they use any surrogate model; such has, Craig-Bampton Reductions, POD, etc.

Acknowledgment

This work was originally printed for the AIAA SDM Conference in 2012. It is being formatted into a SAND Report so that it is properly archived and can be accessible here at Sandia National Laboratories.

Contents

Nomenclature **8**

1 Introduction **9**

2 Surrogate Model Creation Techniques Used for Structural Analysis **11**

3 Surrogate Model Verification **15**

3.1 Response Quantities of Interest (RQI) 15

3.1.1 Windowed Spectral Density (WSD) 15

3.1.2 Input Energy Spectrum (IES) 17

3.2 Model Reduction Methods Technique Verification 17

3.3 Application Verification 19

4 Parametric Uncertainty **27**

5 Conclusions **31**

References **32**

List of Figures

1.1 Overview of QMU process for qualification. 10

2.1 Illustration of modeling to create the Surrogate Model in a Craig-Bampton reduction. A Surrogate Model will be made of Substructure 1. 13

3.1 Windowed Spectral Density (WSD) example using a Gaussian function for the windows. 16

3.2 Creation of a Craig-Bampton surrogate model from a substructure, where blue dots represent the fixed interface constraints. 18

3.3 Richardson extrapolation example of a Craig-Bampton surrogate model with varying fixed interface modes for a modal frequency near 1096 Hz. 19

3.4 Craig-Bampton surrogate models with varying fixed interface modes all show an error less then five percent for a modal frequency up to 2,000 Hz, which is 90 modes. 20

3.5 Full system with two substructures converted to surrogate models. 21

3.6 Comparison of full system with surrogate models to original model up to a frequency of 2,000 Hz, which is 190 modes. 22

3.7 A full system model with surrogate models where a response is examined that is not part of the surrogate models. 22

3.8 Time domain acceleration response comparison of full system with surrogate models and one without surrogate models. 23

3.9 Input Energy Spectrum comparison between full system with and without surrogate models, where the measurement is at a point on the full system that is not internal to a surrogate model. 24

3.10 Input Energy Spectrum comparison between full system with and without surrogate models, where the measurement is at a point that is internal to one of the surrogate models. 25

3.11 Windowed Spectral Density comparison between full system with and without surrogate models, where the measurement is at a point that is internal to one of the surrogate models. 26

4.1 Force input and response measurement points for comparison of parametric uncertainty and errors associated with using surrogate models in the full system. 27

4.2 Windowed Spectral Density comparison between full system with and without surrogate models, where the measurement is at a point that is internal to one of the surrogate models. 28

4.3 Windowed FRF comparison at a response location in substructure two, illustrating that parametric uncertainty bounds the error associated with using surrogate models in the full system. 29

4.4 Windowed FRF comparison at a response location in the section between substructure one and two, illustrating that parametric uncertainty bounds the error associated with using surrogate models in the full system. 30

Nomenclature

$E_I^R(f_n, \xi)$	Input energy spectrum
f	Frequency
G_{xx}	Spectral density of acceleration
$GRMS$	Acceleration RMS
$H_v(f, f_n, \xi)$	Acceleration input, relative velocity output FRF
$R_{xx}(\tau)$	Autocorrelation function
$\sigma^2(f_m)$	Windowed power spectral density
$W(f)$	Absolute integrable function (windowing function)
$\ddot{x}(t)$	Acceleration response
$\ddot{X}(f, \tau)$	Finite Fourier transform

Chapter 1

Introduction

The development of a model is one of the most important parts of performing an analysis of a system. Once the model is created, it is first verified to insure that the mesh is adequately converged providing a numerically stable solution. Next, the model is validated using criteria that depend on its intended use. For a model that is to be used for quick design assessments, validation with low stringency may be done; by contrast, if the model is to be used for system qualification, then an extensive validation program is necessary.

In a large complex system, a full system model can be used to provide component responses given certain full system environments. The component models within the full system model need only be adequate to capture the response at the component. Uncertainties can be and should be included throughout this process to provide a distribution of component responses. An envelop of responses provides the environmental specification (ES) for the component. Once the environmental specification at the component is known, then a more detailed model of the component or an actual test of the component can be driven with this enveloped specification. If the failure mechanism of the component is known or the part is tested to failure, then it is possible to quantify the margins and uncertainty of the component given various full system environmental inputs. This quantification of margins and uncertainties (QMU) process is illustrated in Fig. 1.1.

These analyses can require a large amount of computing resources in number of processors, memory, and wall time; especially, if uncertainty is propagated through the simulation providing a distribution of responses. Here surrogate models of components and subsystems of the full system model can be very advantageous in reducing the computational burden of running a high-order model of the full system. However, it is imperative that the error inherent in using the surrogate model be quantified. In addition, the surrogate model needs to be able to propagate any uncertainties that are relevant to the component response through the simulation.

An important aspect of this process is the quantified loss of fidelity. Any surrogate model will have a loss of fidelity due to the model reduction process. The reduced model can consist of many different submodels that have been reduced using potentially different techniques such as Craig-Bampton formulation [6], Craig-Chang formulation [7], proper orthogonal decomposition [10], or component mode synthesis (CMS) [2, 4]; potentially, some submodels may not be reduced at all and consist of the original finite element (FE) mesh. The unreduced submodels may be where loads are applied or contain regions where uncertainty quantification is to be performed. Each individual reduced component model can be verified as Ladevéze and Chamoin have done for a

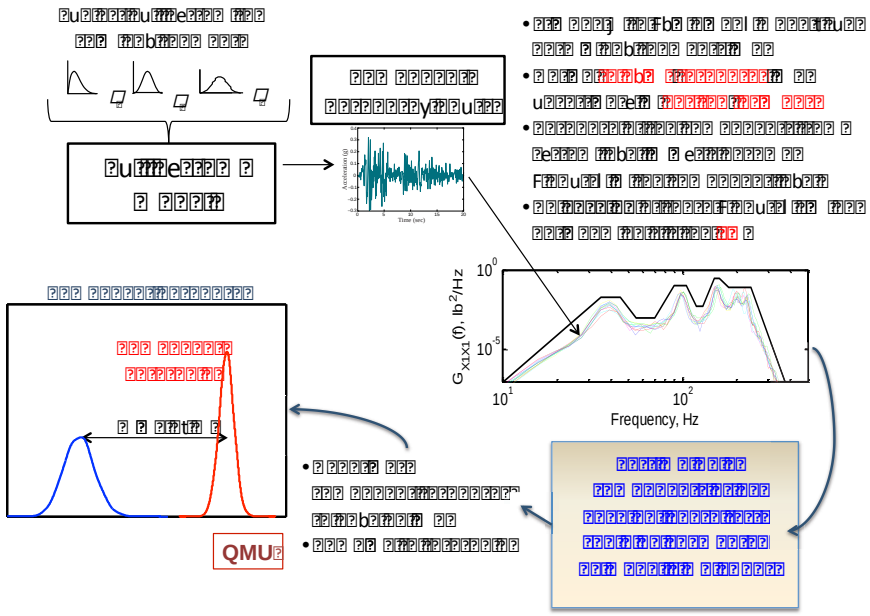

Figure 1.1. Overview of QMU process for qualification.

reduced model using proper generalized decomposition [11]. However, the combination of many reduced component models with some unreduced submodels is more difficult to verify, but equally important. Typically, in structural dynamics applications the reduced model is compared to the high-order model by comparing the natural frequencies of the two models. This also provides a qualitative error assessment of the surrogate model.

This paper addresses the verification of a surrogate model that is used for two main types of environmental loads: a random vibration event and an impulse shock. Examples of a random vibration event include turbulent flow over an aircraft wing and atmospheric re-entry of the shuttle. An example of an impulse shock is observed when a pyrotechnic device fires to release a structural attachment as is the case for stage separation in many launch vehicles. In this work, a high fidelity model of the full system was created; however, the high-order model is computationally intractable when attempting to quantify uncertainties using any sampling procedure. Therefore, a surrogate model was created. This surrogate model is verified in this paper, and the error or uncertainty in using the surrogate model is quantified for the applications of interest: a random vibration event and an impulse shock.

This paper is organized as follows. Section 2 briefly discusses how the surrogate model was created. Section 3 presents the hierarchal technique for verifying the surrogate model for structural analysis. In this section, response quantities of interest are defined to help with the verification. Section 4 discuss the quantification of the error and how uncertainties are propagated through the surrogate model. Finally, the conclusions and recommendations of this paper are presented.

Chapter 2

Surrogate Model Creation Techniques Used for Structural Analysis

There are several techniques for reducing models. They range in complexity from model simplification to the complex where an experimental substructure is attached to the finite element substructure [13]. The work for this project uses three techniques for reducing the size of our model: Craig-Bampton formulation [6], model simplification, and a CMS technique for coupling experimental and analytical models known as the Modal Constraints for Fixtures Subsystems (MCFS) [2, 3, 13]. The focus of the paper is on the Craig-Bampton formulation, for it is the most widely known. However, the procedures describe are applicable to the other two methods.

The structural dynamics simulation tool used in this analysis is Sandia National Laboratories' Sierra Structural Dynamics code. The theory for the Craig-Bampton is taken from the Sierra Structural Dynamics Theory Manual [14]. In the Craig-Bampton method, the model is reduced using fixed interface modes and constraint modes. The method is outlined in some detail in Craig's book [5]. The Craig-Bampton method is typically applied to eigenvalue analysis, but it may be used in other solution methods as well. Here it is only describe in an eigen analysis application.

The entire model of a structure may be reduced to the interface degrees of freedom and generalized degrees of freedom associated with internal modes of vibration. Consider the general eigenvalue problem, with the system matrices partitioned into interface degrees of freedom, V, and the complement, C,

$$\left(\begin{bmatrix} K_{vv} & K_{vc} \\ K_{cv} & K_{cc} \end{bmatrix} - \lambda \begin{bmatrix} M_{vv} & M_{vc} \\ M_{cv} & M_{cc} \end{bmatrix} \right) \begin{bmatrix} u_v \\ u_c \end{bmatrix} = 0. \tag{2.1}$$

In this work only the cases where K_{vv} is nonsingular are considered. For the Craig-Bampton method, this implies that clamping the interface degrees of freedom removes all zero energy modes from the structure.

The Craig-Bampton method reduces the physical degrees of freedom, u, to generalized coordinates, p, using a set of preselected component modes, Ψ,

$$u = \Psi p. \tag{2.2}$$

The component modes are selected as follows. We let $\Psi = [\Phi \ \psi]$, where Φ is a set of eigen

modes of the fixed interface, i.e.,

$$(K_{vv} - \lambda M_{vv})\,\Phi = 0.$$

We retain only a subset of the modes in this system. In addition, we define the constraint modes, ψ, as the static condensation of the problem. Each column of ψ is the solution of the static problem where one interface degree of freedom has unit displacement, and all other interface degrees of freedom are fixed. As shown in Craig [5],

$$\psi = -K_{vv}^{-1} K_{vc}. \tag{2.3}$$

Note that since we require that K_{vv} be positive definite, all these solutions are well defined. The matrix need be factored only once for all of the modes.

The reduced system matrices can be written as

$$\mu = \begin{bmatrix} \mu_{kk} & \mu_{kc} \\ \mu_{ck} & \mu_{cc} \end{bmatrix}, \tag{2.4}$$

and,

$$\kappa = \begin{bmatrix} \kappa_{kk} & \kappa_{kc} \\ \kappa_{ck} & \kappa_{cc} \end{bmatrix}, \tag{2.5}$$

where,

$$\begin{aligned} \mu_{kk} &= I_{kk} \\ \mu_{kc} &= \mu_{ck}^T = \phi^T (M_{vv}\psi + M_{vc}) \\ &= \phi^T M_{vv}\psi + (M_{cv}\phi)^T \\ \mu_{cc} &= \psi^T (M_{vv}\psi + M_{vc}) + M_{cv}\psi + M_{cc} \\ &= \psi^T M_{vv}\psi + (M_{cv}\psi)^T + M_{cv}\psi + M_{cc}, \end{aligned} \tag{2.6}$$

and,

$$\begin{aligned} \kappa_{kk} &= \Lambda_{kk} \\ \kappa_{kc} &= \kappa_{ck} = 0 \\ \kappa_{cc} &= K_{cc} - K_{cv} K_{vv}^{-1} K_{vc} \\ &= K_{cc} + K_{cv}\psi. \end{aligned} \tag{2.7}$$

A natural break between a full finite element model and the surrogate model, especially in the Craig-Bampton CMS technique, is at connection points in the model, such has bolted joints. This can be an arduous task for the modeler, especially if it is desired to capture joint dissipation mechanisms. This is because they have to account for bolt mechanism in the substructure that is being made into a surrogate model.

The models developed for this study contain three substructures that are connected through bolted connections. Two of the three substructures will be made into surrogate models and connected to the remaining substructure to create the full system. A depiction of the modeling methodology is shown in Fig. 2.1. Here a surrogate model will be made of substructure one. It will encompass the stiff spring the rigid elements connecting the stiff spring to substructure one and the FE representation of substructure one. The interface constraint would be at the node connecting the stiff spring to the *Joint2G* [15] element. The *Joint2G* element is used to capture the dissipation mechanisms of the joint.

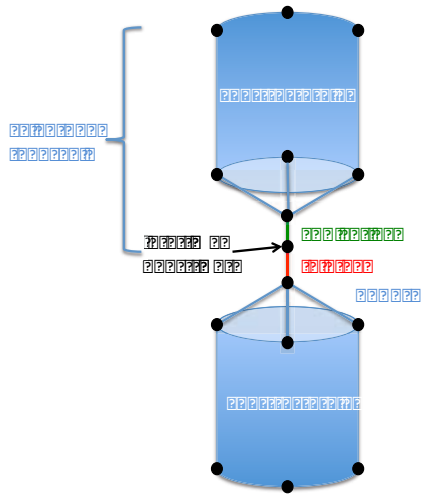

Figure 2.1. Illustration of modeling to create the Surrogate Model in a Craig-Bampton reduction. A Surrogate Model will be made of Substructure 1.

Chapter 3

Surrogate Model Verification

"Verification is the process of determining that a model implementation accurately represents the developer's conceptual description of the model and the solution to the model." [1]. The surrogate model can be verified and error quantified when comparing to the high fidelity (or high-order) model as done by Lieu et al. [12]. Implicit in this is that the high fidelity model has already been verified. In this section we define a hierarchal approach to minimize the error associated with using the surrogate model. The first step in this process is technique verification in the creation of the surrogate models. Next, the subsystems that are reduced are verified in a modal sense. Then, the full system surrogate model is verified to the high-order model in a modal sense. Finally, the surrogate model is verified in regards to the applications of interest: a random vibration event and an impulse shock. Before the verification can begin response quantities of interest need to be defined.

3.1 Response Quantities of Interest (RQI)

Response Quantities of Interest (RQI) are defined to help in the verification and quantification of error for the surrogate model. Basic structural dynamics quantities, natural frequencies and mode shapes, will be used where appropriate. In addition, a Windowed Power Spectral Density (WPSD) and the input energy spectrum (IES) will be used as RQI. These are defined in the subsections 3.1.1 and 3.1.2.

3.1.1 Windowed Spectral Density (WSD)

The spectral density (SD) in a practical sense provides the mean square frequency content for a stationary and random process. The spectral density is also called the auto-spectral density (ASD) and is defined as the Fourier transform of the autocorrelation function, $R_{xx}(\tau)$,

$$G_{xx}(f) = 2\int_{-\infty}^{\infty} R_{xx}(\tau)e^{-j2\pi f\tau}d\tau,\ f \geq 0, \tag{3.1}$$

where τ is a finite time period, f is the frequency, and $j = \sqrt{-1}$. Following the development given by Wirsching et al. [17], one can show for a given acceleration response, $\ddot{x}(t)$, that is stationary

that

$$G_{xx}(f) = \lim_{T\to\infty} \frac{1}{2\pi T} \boldsymbol{E}[|\ddot{X}(f,T)|^2], \tag{3.2}$$

where $\boldsymbol{E}[\cdot]$ denotes the expected value, and $\ddot{X}(f,\tau)$ is the finite Fourier transform of the given acceleration response ($\ddot{x}(t)$).

To use the SD as a validation metric, a sequence of windows is defined that span the frequency ranges of interest or frequency bands within the spectral density. Next the spectral density is multiplied by a windowing function, $W(f)$ and integrated over that band of interest. An example of a windowing function could be a Gaussian function or may be just unity. Therefore, the windowd spectral density (WSD) is given as

$$\sigma^2(f_m) = \int_{f_i}^{f_{i+1}} G_{xx}(f)W(f)df, \tag{3.3}$$

where $W(f)$ is a nonnegative, absolutely integrable function (windowing function), $G_{xx}(f)$ is the SD, f_m is the centroid of an evenly spaced frequency interval, f_i is the beginning of the frequency interval, and f_{i+1} is the end of the frequency interval. The windowing functions in this study are Gaussian densities with centers at frequencies of interest, e.g., modal frequencies. This is very similar to work by Urbina et al. [16], except the SD is used in place of the transfer function. This provides a scalar value at the medium frequency for the frequency interval f_i to f_{i+1}. This process is illustrated in Fig. 3.1.

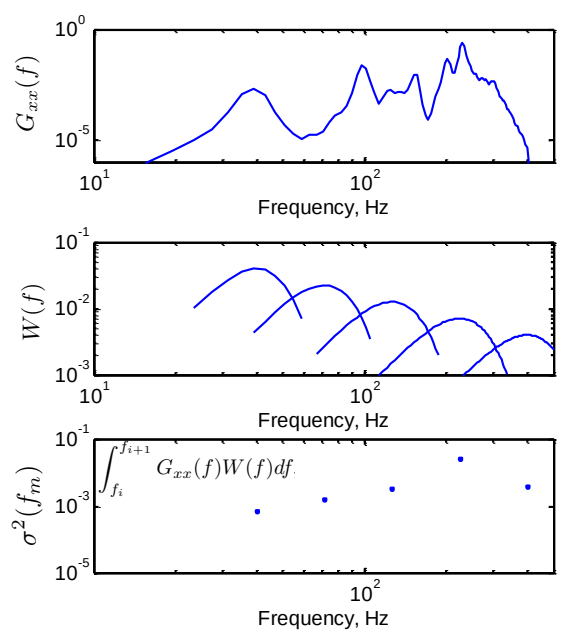

Figure 3.1. Windowed Spectral Density (WSD) example using a Gaussian function for the windows.

A physical interpretation is that the quantity defined in Eq. 3.3 is a weighted mean square of the random process with spectral density $G_{xx}(f)$. When the weighting function is unity and the square root of Eq. 3.3 is computed we obtain the mean root-mean-square contribution to the random process in the interval $[f_i, f_{i+1}]$.

3.1.2 Input Energy Spectrum (IES)

The Input Energy Spectrum (IES) is also a method to assess the frequency content of a response or in a component sense the frequency content of the input [9]. The full system model will generate responses that are inputs to the components. The IES is also an attractive alternative to the typical Shock Response Spectrum (SRS) for shock analysis [9].

The basic equation of the IES for a single degree of freedom (SDOF) oscillator is given as

$$\frac{E_I^R(f_n,\xi)}{m} = \int_{-\infty}^{\infty} |\ddot{X}(f)|^2 Re[H_v(f,f_n,\xi)]df, \tag{3.4}$$

where $\ddot{X}(f,\tau)$ is the finite Fourier transform of the given acceleration response ($\ddot{x}(t)$), τ is a finite time period, and $H_{v,j}(f)$ is an acceleration input, relative velocity output FRF. This FRF is mathematically defined as

$$H_v(f,f_n,\xi) = \frac{-jf}{f_n^2 - f^2 + 2j\xi f_n f}, \tag{3.5}$$

where f_n is the natural frequency, and ξ is the damping factor. In Eq. (3.4) it is assumed that the response acceleration is the input to the SDOF oscillator. This is a valid assumption for the work of the full system model, since the response of the full system model is generally an input to a component model.

This method is similar to the WSD. Instead of the acceleration being converted into a spectral density and then multiplied by a windowing function, the acceleration is Fourier transformed and then multiplied by a windowing function. The windowing function $W(f)$ is the term $Re[H_v(f,f_n,\xi)]$.

3.2 Model Reduction Methods Technique Verification

In Section 2, three main methods for creating the surrogate model were mentioned: Craig-Bampton model CMS, model simplification, and a CMS technique for coupling experimental and analytical models. This section discusses methods to assure that the techniques for creating the reduced surrogate models are accurate. First, the surrogate model's modal frequencies are compared to the modal frequencies of the actual substructure model from which the surrogate model was created. Then, the surrogate model is combined with other full model substructures and again modal frequencies are compared to the full high order model that does not contain any surrogate models.

The analyst has the ability in the Craig-Bampton CMS technique to pick the number of fixed interface modes. The key to selecting the number of interface modes is to assure that the surrogate

model is capable of capturing up to the frequency of interest. However, for model efficiency, the analyst should keep the number of selected fixed interface modes to a reasonable number. In the Sierra Structural Dynamics code with a multi-processor run, the surrogate model is restricted to a single processor. Thus, it has a size constraint of memory on the processor as well. An example surrogate model from a substructure is depicted in Fig. 3.2.

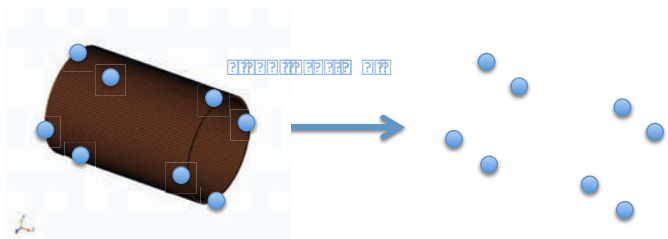

Figure 3.2. Creation of a Craig-Bampton surrogate model from a substructure, where blue dots represent the fixed interface constraints.

Three different surrogate models of the same subsystem are created with the difference between them being the number of fixed interface modes selected. An eigen solution is performed on each surrogate model. At each mode shape, the modal frequencies of the three models are used in a Richardson extrapolation method to determine a converged modal frequency solution. In order for a surrogate model to be accepted it must be within two percent of the Richardson extrapolation converged modal frequency up to the frequency of interest. An example of a Richardson extrapolation for a surrogate model with varying fixed interface modes is shown in Fig 3.3.

In addition, the modal frequency of the selected surrogate model must be within five percent of the same subsystem's modal frequency determined from its full FE model. This is also important up to the frequency of interest. Figure 3.4 illustrates that three different surrogate models made with varying number of interface modes (100, 200, and 300 modes) all produce an error compared to the full substructure model under five percent up to 2,000 Hz.

The above was conducted to confirm that the creation of the surrogate model worked and that the analyst selected an appropriate amount of fixed interface constraint modes for the surrogate. Next, the created surrogate model is verified in the complete system. In a very similar manner, this is accomplished by comparing a full system high-order model to a full system model with surrogate substructures. The comparison is made using the modal frequencies.

In the full system, there may be multiple surrogate models. The models are first verified individually and then all the surrogate models are compared against the full system high fidelity model. For brevity, the full system is compared with the two surrogate models in the example, seen in Fig. 3.5.

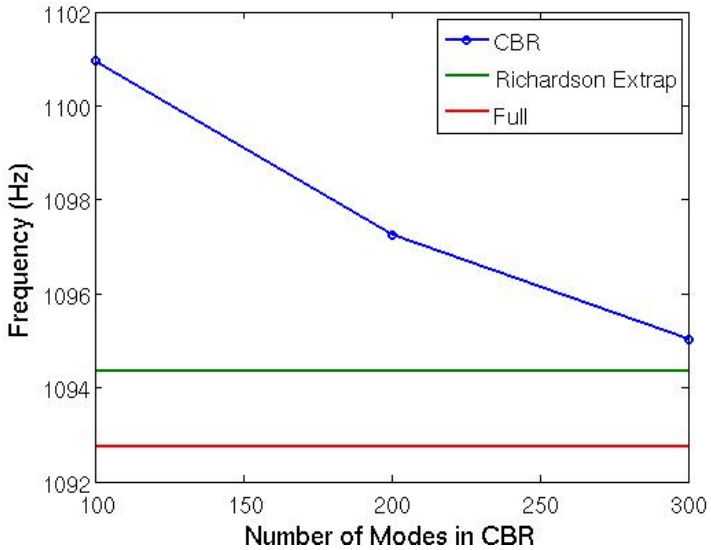

Figure 3.3. Richardson extrapolation example of a Craig-Bampton surrogate model with varying fixed interface modes for a modal frequency near 1096 Hz.

Once again, a different number of interface constraint modes are selected for the surrogate models created by the Craig-Bampton method. In order for a surrogate model to be accepted it must be within two percent of the Richardson extrapolation converged modal frequency up to the frequency of interest. Also, the modal frequency of the full system with the surrogate model must be within five percent of the full system's modal frequency determined from its full FE model or experimentation up to the frequency of interest. Figure 3.6 illustrates that the surrogate models of substructure one and two could be made with 100 interface constraint modes and be acceptable for a frequency of interest up to 2,000 Hz.

3.3 Application Verification

The next level of verification is to compare the quantities of interest for the surrogate model and high-order model. The concept is to drive the models with pseudo representative application loads. The first application is an impulse shock load. The second application to represent is a random vibration event.

The impulse shock load is represented with a haversine shaped pulse, $A(t)_{HAV}$.

$$A(t)_{HAV} = \begin{cases} 0.5A_{peak}\left\{1 \quad cos\left(\frac{2\pi t}{T_{BASE}}\right)\right\}, & \text{for } 0 < t < T_{BASE} \\ 0, & \text{otherwise.} \end{cases} \tag{3.6}$$

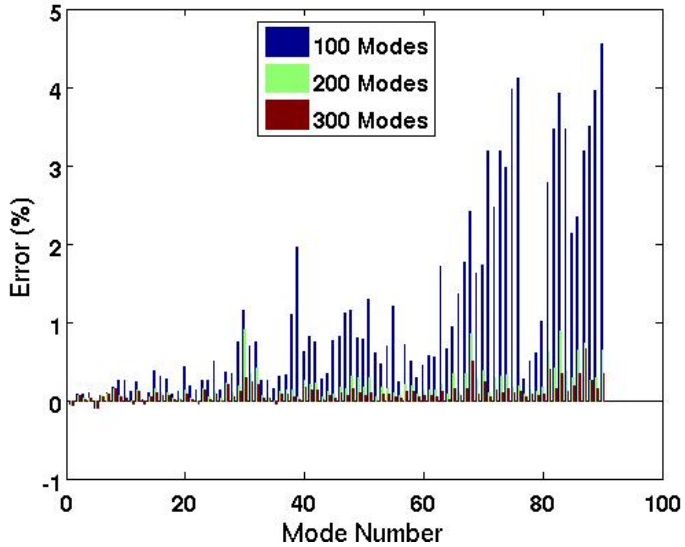

Figure 3.4. Craig-Bampton surrogate models with varying fixed interface modes all show an error less then five percent for a modal frequency up to 2,000 Hz, which is 90 modes.

The comparisons should be made at degrees of freedom on the boundary of a submodel, typical instrumented flight test locations, and at internal degrees of freedom in the surrogate model. The internal degrees of freedom are important to verify as these degrees of freedom require a transformation in order to extract their response. By using interface, internal, and typical flight test locations, the transformation between the high-order model and the surrogate model will be verified.

There will be some differences between the various metrics for both the high-order model and the surrogate model. The amount of acceptable variation must be defined to ensure that surrogate model adequacy can be defended. In a shock environment, the preferred metric is the IES as discussed by Edwards [8, 9]. The goal for the comparison between the full system with surrogate models and the full system without is for the IES not to exceed ± 6 dB over 100% of the frequency range of interest, and for it not to exceed ± 3 dB over 80% of the frequency range of interest. The frequency range of interest in this study is 2,000 Hz. This is similar to experiment specifications and it would be inappropriate for the model to be expected to perform better than experiments.

The first comparison is on a portion of the full system that is not part of a surrogate model as in Fig. 3.7. The acceleration responses are shown in Fig. 3.8. The IES comparison is shown in Fig. 3.9, where 90% are less then ± 3 dB and 100% are less then ± 6 dB. The second comparison is at a measurement location internal to the surrogate model. The IES comparison is shown in Fig. 3.10, where 80% are less then ± 3 dB and 100% are less then ± 6 dB. Therefore, the surrogate models used in the full system for shock environments are verified.

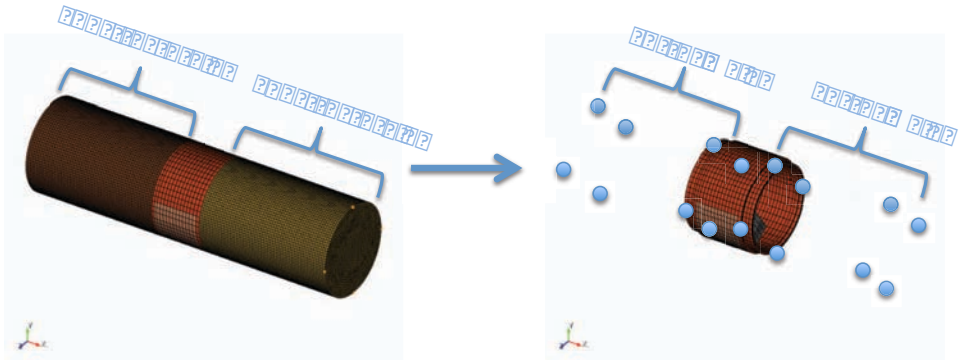

Figure 3.5. Full system with two substructures converted to surrogate models.

To simulate the random vibration environment, both the surrogate and the high-order model are driven with broadband noise with a bandwidth equal to the maximum frequency of interest. In a random vibration environment, the WSD is believed to be a better verification metric. The goal for verification is for the WSD not to exceed $\pm 6\ dB$ over 100% of the frequency range of interest, and for it not to exceed $\pm 3\ dB$ over 80% of the frequency range of interest.

Once again, the comparisons should be made at degrees of freedom on the boundary of a submodel that should pass through the model reduction transformations and be predicted identically in both models, at degrees of freedom that are internal to the submodels that would require a transformation in order to extract their response, and at typical flight test locations. The surrogate models created as an example for this study were verified for both surrogate model internal measurements and measurements for a portion of the model that is not created from a surrogate model. The WSD comparison for a measurement internal to a surrogate model is shown in Fig. 3.11, where 90% are less then $\pm 3\ dB$ and 100% are less then $\pm 6\ dB$. Therefore, the surrogate models used in the full system for random vibration environments are verified.

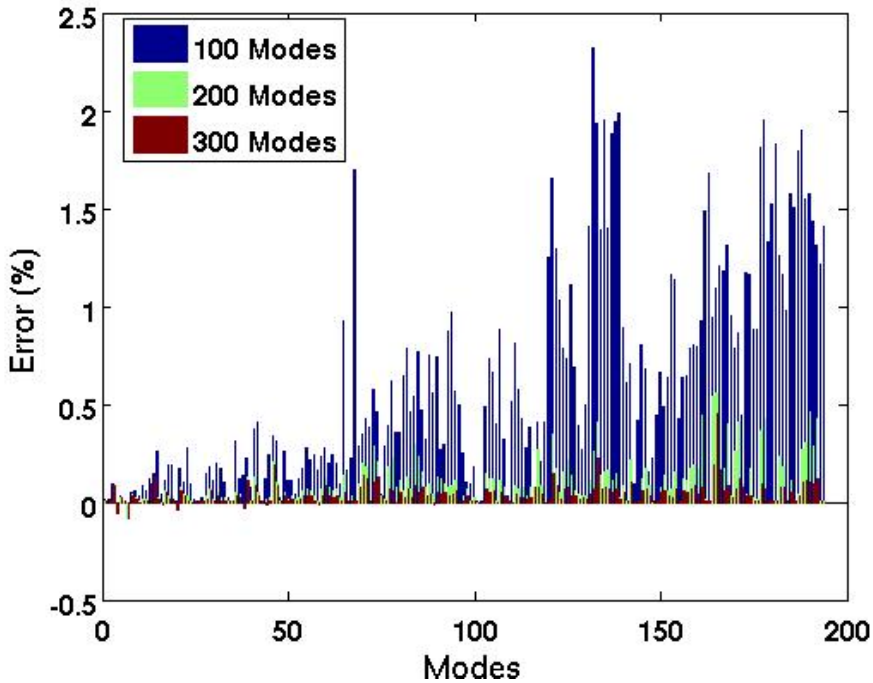

Figure 3.6. Comparison of full system with surrogate models to original model up to a frequency of 2,000 Hz, which is 190 modes.

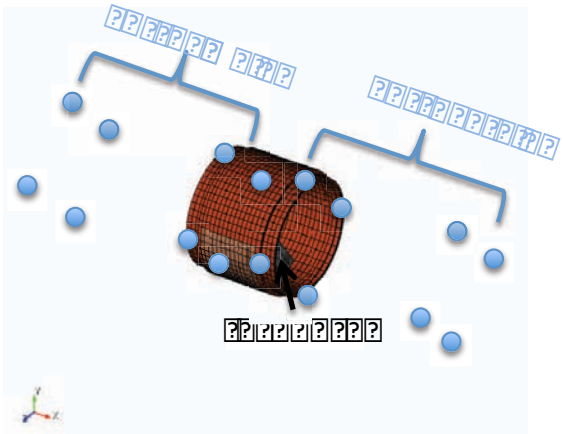

Figure 3.7. A full system model with surrogate models where a response is examined that is not part of the surrogate models.

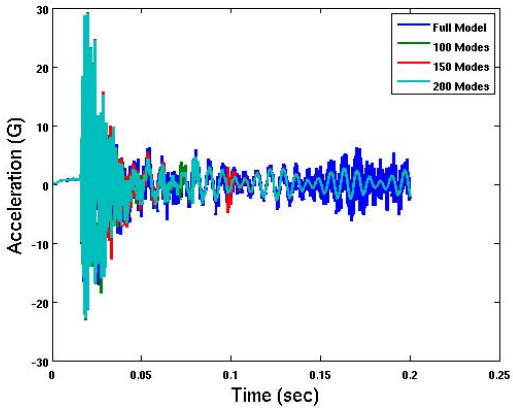

Figure 3.8. Time domain acceleration response comparison of full system with surrogate models and one without surrogate models.

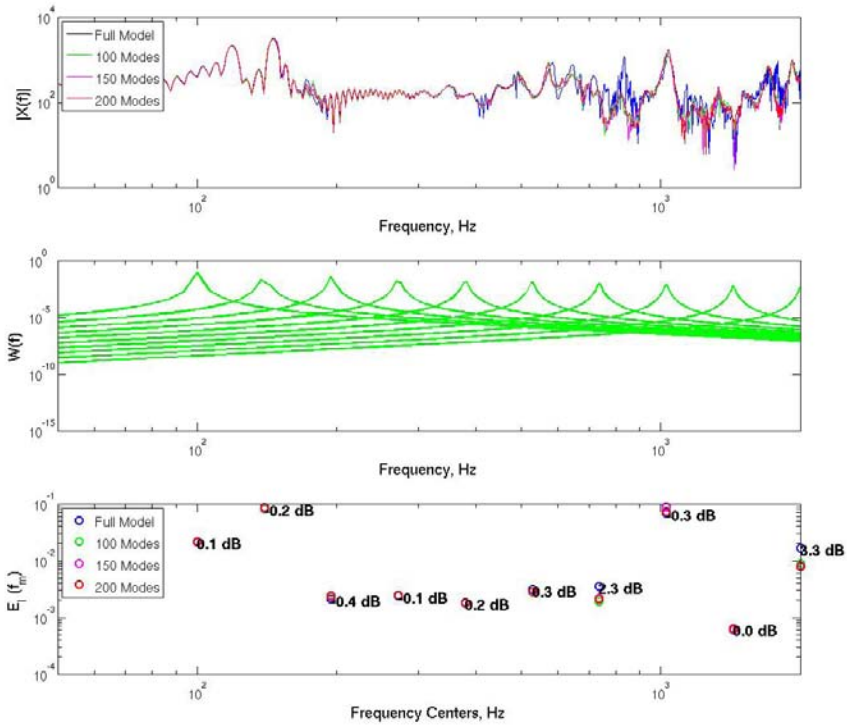

Figure 3.9. Input Energy Spectrum comparison between full system with and without surrogate models, where the measurement is at a point on the full system that is not internal to a surrogate model.

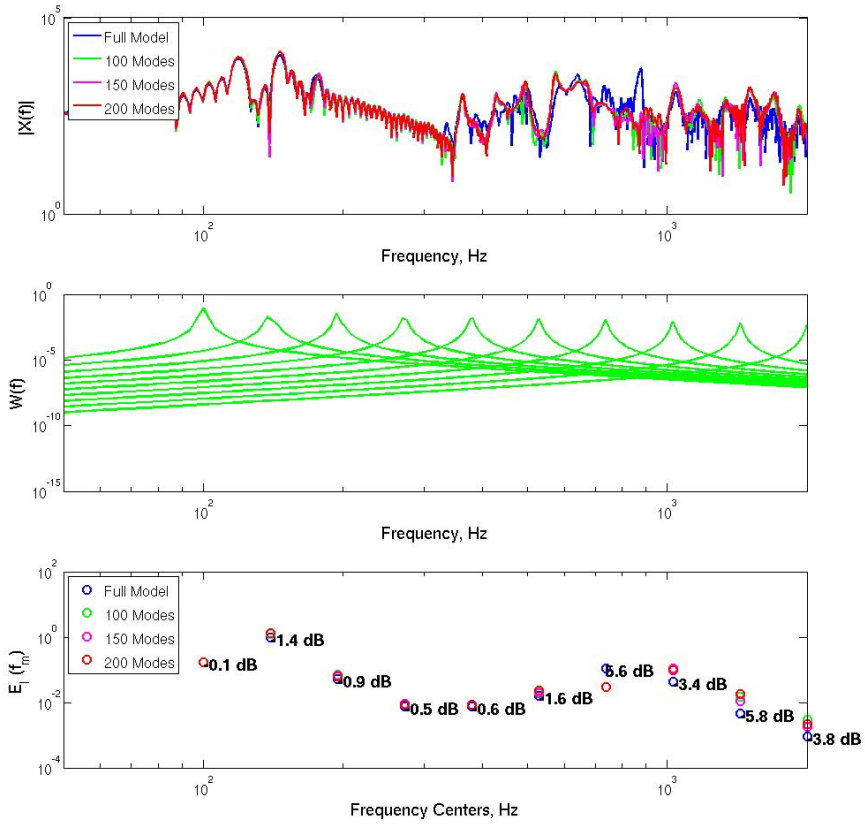

Figure 3.10. Input Energy Spectrum comparison between full system with and without surrogate models, where the measurement is at a point that is internal to one of the surrogate models.

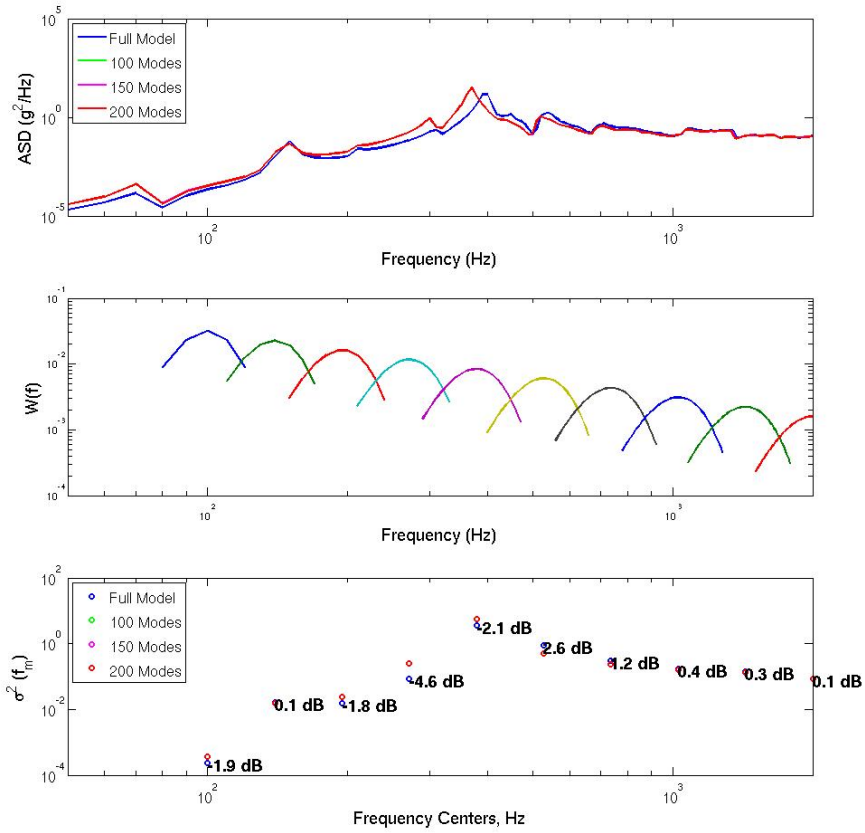

Figure 3.11. Windowed Spectral Density comparison between full system with and without surrogate models, where the measurement is at a point that is internal to one of the surrogate models.

Chapter 4

Parametric Uncertainty

This section discusses the effect of the error using the surrogate models in the full system as compared to parametric uncertainty. It is found that the parametric uncertainty completely bounds the error associated with using the surrogate models in the full system for an application of shock. The shock is characterized with a modal hammer at the force input and responses measurement locations as shown in Fig.4.1. It is important to recognize that the model is validated and the uncertainty is quantified using the surrogate models in the system.

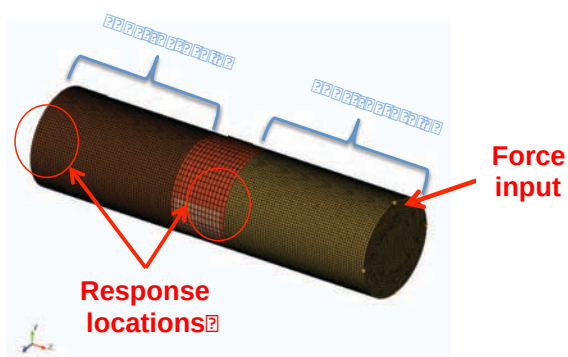

Figure 4.1. Force input and response measurement points for comparison of parametric uncertainty and errors associated with using surrogate models in the full system.

The parametric uncertainty is accounted for in the joints, the full system damping, and a silicon pad material used for vibration isolation between an instrumentation box and the structure. The system studied has two main joints between substructure one and middle section and the middle section and substructure two, as seen in Fig. 4.2. These joints are characterized by parametric uncertainty where the axial and rotational stiffness is varied from $0.7x10^7$ to $1.3x10^7$ lbf/in with a uniform distribution. The damping in the system is also characterized by full system mass and stiffness proportional Raleigh damping where the α and β coefficients are varied from $0.5x10^{\ 6}$ to $5.0x10^{\ 6}$ and $1x10^{\ 4}$ to $10x10^{\ 4}$, respectively, with a uniform distribution. The silicon pad's modulus of elasticity is varied from 700 to 1300 *psi* with a uniform distribution. Finally, the silicon

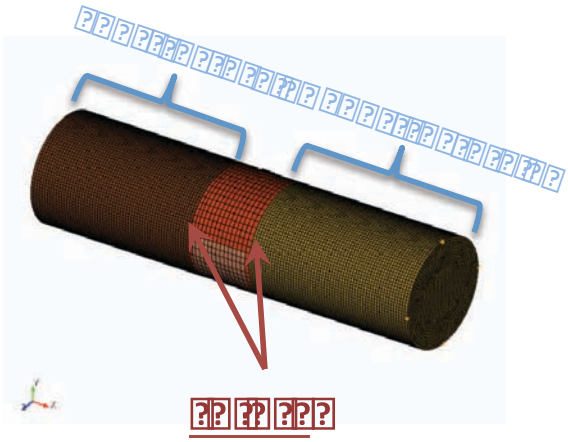

Figure 4.2. Windowed Spectral Density comparison between full system with and without surrogate models, where the measurement is at a point that is internal to one of the surrogate models.

pad's Poissons ratio is varied from 0.45 to 0.4999 with a uniform distribution.

A windowed FRF (frequency response function) comparison is used to illustrate that the parametric uncertainties bound the error associated with using the surrogate models. The windowed FRF is identical to the windowed spectral density; except the spectral density is replaced with the FRF. Eighty Latin Hypercube Sample (LHS) realizations of the random variables were used to compute the distribution of the windowed FRF at specific frequencies. The results are shown in Fig. 4.3 for the response in substructure 2 and Fig. 4.4 for the other response location. As can be seen the parametric uncertainty completely bounds any error associated with using surrogate models in the full system.

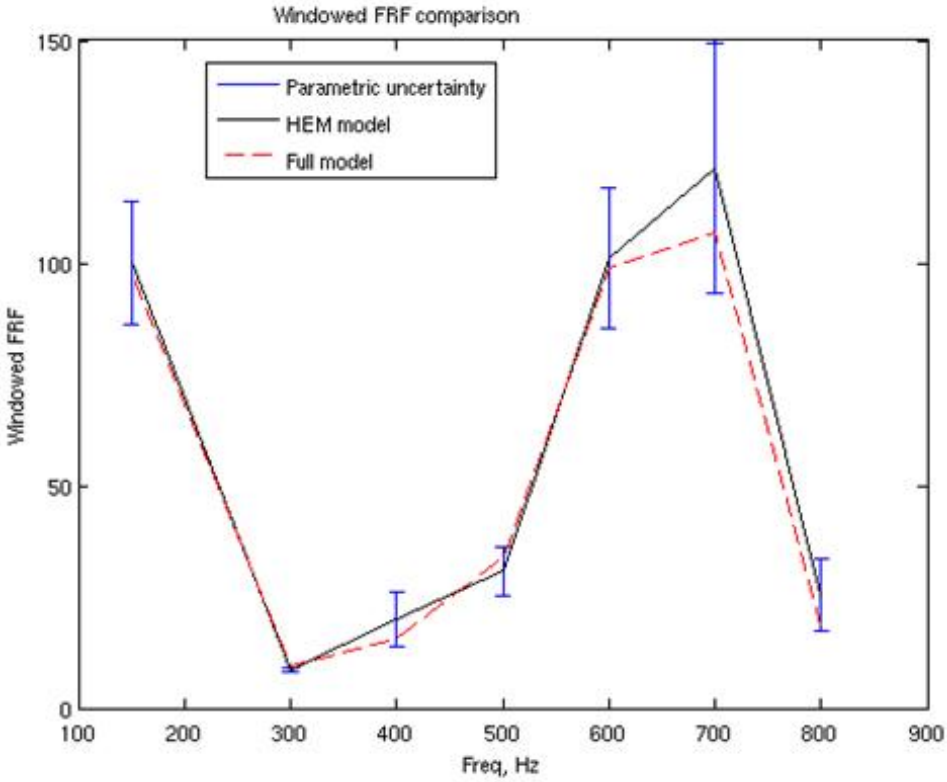

Figure 4.3. Windowed FRF comparison at a response location in substructure two, illustrating that parametric uncertainty bounds the error associated with using surrogate models in the full system.

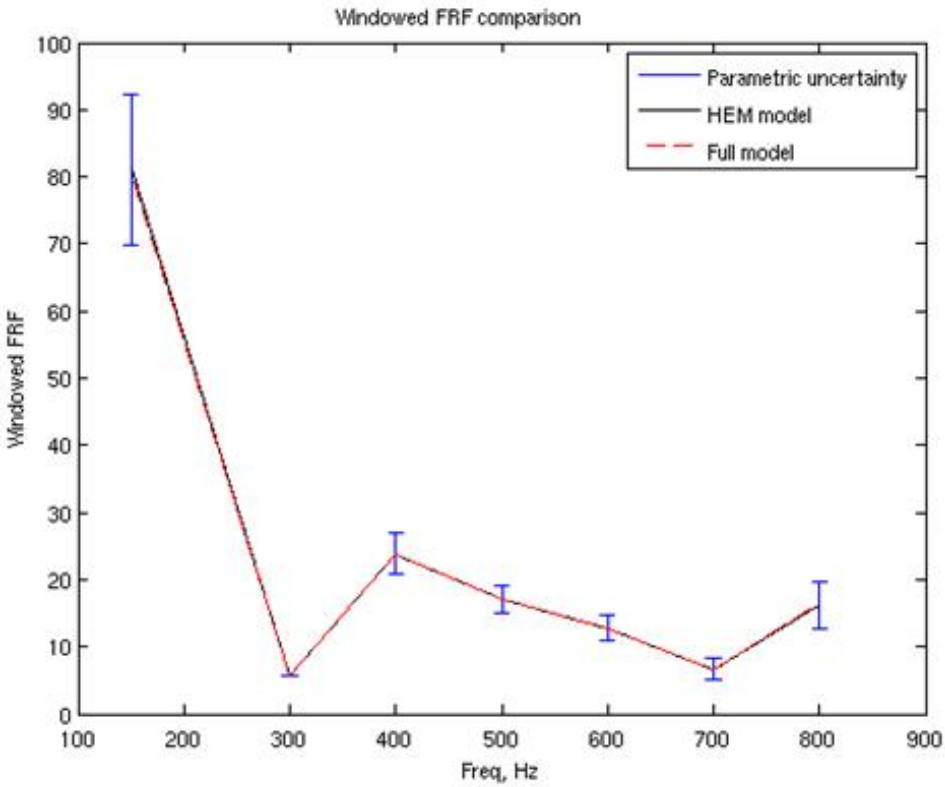

Figure 4.4. Windowed FRF comparison at a response location in the section between substructure one and two, illustrating that parametric uncertainty bounds the error associated with using surrogate models in the full system.

Chapter 5

Conclusions

Model reduction is generally accomplished by creating surrogate models from a high-fidelity model. These surrogate models are generally created from techniques that utilize a reduced basis to recreate the dominant behavior of the system to be modeled. Unfortunately, this reduced basis comes at a cost of model accuracy. Therefore, this paper first verifies that the model reduction is sufficient for structural dynamics analysis of a random vibration event and an impulse shock load. Second, this paper shows that the error with using the surrogate model is bound by parametric uncertainty. The understanding of the parametric uncertainties is then used in part two of this series of papers for validation of the model and quantifying the margins and uncertainty in this environment.

References

[1] AIAA. Guide for the verification and validation of computational fluid dynamics simulations. Technical Report G-007-1998, American Institute of Aeronautics and Astronautics, 1998.

[2] M. S. Allen, R. L. Mayes, and E. J. Bergman. Experimental modal substructuring to couple and uncouple substructures with flexible fixtures and multi-point connections. *J Sound Vib*, (329):4891–4906, 2010.

[3] M.S. Allen and R.L. Mayes. Comparison of frf and modal methods for combining experimental and analytical substructures. Odalndo, FL, 2007. 25th International Modal Analysis Conference, IMAC XXV.

[4] W.A. Benfield and R.F. Hruda. Vibration analysis of structures by component mode substitution. *AIAA*, 9(7):1255–1261, 1971.

[5] R. R. Craig. *Structural Dynamics: An Introduction to Computer Methods*. John Wiley & Sons, 1981.

[6] R. R. Craig and M.C. Bampton. Coupling of substructures for dynamic analyses. *AIAA*, 6(7):1313–1319, 1968.

[7] R. R. Craig and C. J. Chang. Free-interface methods of substructure coupling for dynamic analysis. *AIAA*, 14(11):1633–1635, 1976.

[8] Timothy S. Edwards. Power delivered to mechanical systems by random vibrations. *Shock and Vibration*, 16(3):261–271, 2009.

[9] Timothy S. Edwards. Using work and energy to characterize mechanical shock. *Shock and Vibration*, 2011. submitted for publication.

[10] I.T. Jolliffe. *Principal Component Analysis*. Springer, 2nd edition, 2002.

[11] Pierre Ladevéze and Ludovic Chamoin. On the verification of model reduction methods based on the proper generalized decomposition. *Computer Methods in Applied Mechanics and Engineering*, 200:2032–2047, 2011.

[12] T. Lieu, C. Farhat, and M. Lesoinne. Pod-based aeroelastic analysis of a complete f-16 configuration: Rom adaptation and demonstration. *AIAA Paper 2005-2295*, 2005.

[13] Randy L. Mayes and Michael R. Ross. Advancements in hybrid dynamic models combining experimental and finite element substructures. *Mechanical Systems and Signal Processing*, Accepted for publishing.

[14] Garth Reese, Manoj Bhardwaj, and Timothy Walsh. Salinas- theory manual. Technical Report SAND2009-0748, Sandia National Laboratories, Albuquerque, New Mexico 87185 and Livermore, California 94550, 2009.

[15] Garth Reese, Manoj Bhardwaj, and Timothy Walsh. Salinas- user's notes. Technical Report SAND99-2801, Sandia National Laboratories, Albuquerque, New Mexico 87185 and Livermore, California 94550, 2012.

[16] Angel Urbina, Thomas L. Paez, and David O. Smallwood. A hierarchy of validation measures for structural dynamics. Technical report SAND05-7048C, Sandia National Laboratories, Albuquerque, New Mexico 87185 and Livermore, California 94550, 2005.

[17] Paul H. Wirsching, Thomas L. Paez, and Keith Ortiz. *Random Vibrations: Theory and Practice*. Dover Books, 1995.

DISTRIBUTION:

1	MS MS-0840	Justine Johannes, 1520
1	MS MS-0557	Todd Simmermacher, 1523
1	MS MS-0828	Walt Witkowsku, 1544
1	MS MS-0346	Lili Akin, 1523
1	MS MS-0847	Marcus Billings, 1523
1	MS MS-0847	James Freymiller, 1523
1	MS MS-0346	Tyler Garrett, 1523
1	MS MS-0346	Michael Guthrie, 1523
1	MS MS-0346	Wil Holzmann, 1523
1	MS MS-0836	Luba Kmetyk, 1523
1	MS MS-0346	Mikhail Mesh, 1523
1	MS MS-0557	Jerry Rouse, 1523
1	MS MS-0847	Nebojsa Sebastijanovic, 1523
1	MS MS-0346	Greg Tipton, 1523
1	MS MS-0346	Ryan Schultz, 1523
1	MS MS-0828	Amalia Black, 1544
1	MS MS-0828	Brian Carnes, 1544
1	MS MS-0897	Kevin Copps, 1544
1	MS MS-0386	Kevin Dowding, 1544
1	MS MS-0828	Rich Hill, 1544
1	MS MS-0828	Kenneth Hu, 1544
1	MS MS-0828	Melanie Hubka, 1544
1	MS MS-0828	John Red-Horse, 1544
1	MS MS-0812	Vicente Romero, 1544
1	MS 0899	Technical Library, 9536 (electronic copy)

Sandia National Laboratories